

## OPTICAL MODES OF A DISPERSIVE PERIODIC NANOSTRUCTURE

Gandhi Alagappan\* and Alexei Deinega

Department of Physics, University of Toronto, 60 St. George Street, Toronto, Ontario, M5S 1A7, Canada

**Abstract**—We show that the optical modes of a periodic nanostructure with frequency dependent dielectric constant (i.e., a dispersive optical nanostructure), in general can be written as an ordinary eigenvalue problem of a “dielectric function operator”, for each distinct symmetry representation of the periodic nanostructure. For a frequency dependence in the form of polynomial rational function, the problem translates to a polynomial eigenvalue equation in the frequency of the mode. The resulting problem can be solved using the basis functions of a dielectric backbone structure, which has a frequency independent dielectric constant. Rapid convergence is achieved when the basis functions are selected to be the modes of a dielectric backbone structure that minimizes the frequency perturbation of the dielectric function of the optical nanostructure. In particular, using a two dimensional photonic crystal constructed with a polar crystal as an example, we demonstrate that, remarkable simple cubic equations are sufficient to obtain accurate descriptions of eigenfrequencies.

### 1. INTRODUCTION

Self-assembled (quantum dots [1,2], graphene nanodomains [3,4], or metal-organics frameworks [5,6]) and artificial nanostructured materials (photonic crystals (PCs) [7–10] and metamaterials [11,12]) have been subject of a great interest in recent years due to their properties to manage the light propagation. Their usage brings new perspectives to optoelectronics [13], laser applications [14], plasmonics [15], telecommunication techniques [16], and other practical areas. Efficient computational methods are required to model optical properties of periodic nanostructured materials and to optimize their

---

*Received 9 April 2013, Accepted 8 May 2013, Scheduled 17 May 2013*

\* Corresponding author: Gandhi Alagappan (alagapp@physics.utoronto.ca).

geometry. Eigenmode decomposition is very popular tool to analyze electromagnetic fields arbitrary periodic nanostructures.

Eigenmode decomposition can be carried out using direct or indirect methods. In the indirect methods, the frequency of the optical mode is not a part of the eigenvalue of the mathematical formulation, or involve secondary steps to extract the mode frequencies. In the direct method, the problem is formulated such that the frequencies and the modes of the optical system can be directly extracted from the eigenvalues and the eigenmodes of the mathematical formulation.

Examples of indirect methods include finite difference time domain (FDTD) [17, 18], transfer matrix [19–21] (TM), a combination of FDTD and TM methods [22], and an indirect formulation of plane wave expansion (PWE) method [23–27]. In the indirect PWE, one formulate wavevector components of light to be eigenvalues for a given frequency. The indirect methods are in general time consuming, and often involves scanning of the entire frequency spectrum to locate the eigenmodes of the optical system.

The most popular and direct eigenmode decomposition method, especially in the case of photonic crystals [PCs], is a direct formulation of PWE, where frequency and the modes appear naturally as eigenvalues and eigenmodes of the optical system. Direct formulation of PWE has been used in computations of photonic band gaps [10, 28, 29], equal frequency surfaces for the theory of light refraction and diffraction [30–33], Bragg transmittance and reflectance [10, 34], and spontaneous emission in a PC [35, 36]. Conventionally, direct formulation of PWE handles only nondispersive materials. Few extensions have been made into direct PWE to accommodate the dispersive materials. These include direct PWE formulations for PCs constructed with lossless metals [37], metals with dissipations [38], polar crystals [39, 40], and superconducting composite [41]. Direct eigenvalue formulations also have been carried using the methods of auxiliary field for metamaterials and PCs made of materials with Lorentzian form of dielectric functions [42].

In this paper, we present a new direct approach for eigenmode decomposition in a dispersive periodic nanostructure (DPN). A DPN has frequency and position dependent dielectric constant. We showed that the eigenmodes and the eigenfrequencies of the DPNs, in general can be written as an eigenvalue problem of a newly defined “dielectric function operator”, for each distinct symmetry representation of the eigenmode. This eigenvalue problem can be solved graphically, or upon specific polynomial (or polynomial rational) form of a dielectric function, can be transformed to a polynomial eigenvalue problem in the frequency of the optical mode. It is worth to mention, that in

principle one can model the dielectric functions of any given material by polynomial rational functions or at least by fitting, and therefore the method is suitable for variety of dielectric functions with varying frequency dependence.

The polynomial eigenvalue problem can be solved using a suitable set of basis functions. In the case of PCs, the set basis functions can be set of plane waves or set of Bloch modes of a PC constructed with non-dispersive materials. The latter selection of the basis functions often leads to a rapid convergence and gives a semi-analytical description for the eigenfrequencies and eigenmodes of the DPN. Specifically we showed that the roots of a simple cubic equation accurately yield the eigenfrequencies of a 2D PC constructed with polar crystals. The nature of the analytical roots of the cubic equation explains the appearance of dispersionless bands in the photonic band structure of 2D PCs with polar crystals [39, 40, 43]. The capability of producing semi-analytical results is a feature that is missing in the previous formulations which always involve heavy numerical calculations.

## 2. THEORETICAL FORMALISM

The modes of a DPN is described by a three dimensional time independent wave equation,

$$\nabla \times \nabla \times \mathbf{E}(\mathbf{r}) - \frac{\omega^2}{c^2} \varepsilon(\mathbf{r}, \omega) \mathbf{E}(\mathbf{r}) = 0, \quad (1)$$

where  $\mathbf{r}$ ,  $\omega$ ,  $\mathbf{E}(\mathbf{r})$ , and  $c$  are position vector, light frequency, electric field, and the speed of light respectively. Let's write the dielectric constant of the DPN as  $\varepsilon(\mathbf{r}, \omega) = \varepsilon_{bb}(\mathbf{r}) + \chi(\mathbf{r}, \omega)$ , where  $\varepsilon_{bb}(\mathbf{r})$  and  $\chi(\mathbf{r}, \omega)$  are the frequency independent and the frequency dependent portion of the dielectric constant, respectively. The dielectric geometry described  $\varepsilon_{bb}(\mathbf{r})$  is defined as the dielectric backbone structure. Note that the dielectric backbone can be either a non-dispersive homogenous medium, vacuum or complex nanostructure (such as a PC) constructed with frequency independent dielectric materials. In order to solve Equation (1), let's expand the electric field using a set of basis functions,

$$\mathbf{E}(\mathbf{r}) = \sum_m f_m \phi_m(\mathbf{r}), \quad (2)$$

where  $\phi_m(\mathbf{r})$ , is the basis function of label —  $m$ . We can take the basis functions as solutions to Equation (1) when  $\chi(\mathbf{r}, \omega) = 0$  (i.e., the modes of the dielectric backbone structure). The basis function satisfies,

$$\nabla \times \nabla \times \phi_m(\mathbf{r}) - \frac{\omega_m^2}{c^2} \varepsilon_{bb}(\mathbf{r}) \phi_m(\mathbf{r}) = 0, \quad (3)$$

where  $\omega_m$  represents the frequency of the  $m$ -th basis function. The basis functions also satisfy the orthogonality relationship,

$$\frac{1}{V} \int_{unit\ cell} \phi_n^*(\mathbf{r}) \varepsilon_{bb}(\mathbf{r}) \phi_m(\mathbf{r}) d^3\mathbf{r} = \delta_{nm}, \quad (4)$$

where  $V$  is the volume of the unit cell.

Substituting Equation (2) into Equation (1) and using Equation (3), we have  $\sum_m f_m [\frac{\omega_m^2 - \omega^2}{c^2} \varepsilon_{bb}(\mathbf{r}) \phi_m - \frac{\omega^2}{c^2} \chi(\mathbf{r}, \omega) \phi_m] = 0$ . Multiplying this equation with  $\phi_n^*(\mathbf{r})$ , and applying the orthogonality relationship in Equation (4), we obtain,

$$(\omega_n^2 - \omega^2) f_n = \frac{\omega^2}{V} \sum_m f_m \int_{unit\ cell} \phi_n^*(\mathbf{r}) \chi(\mathbf{r}, \omega) \phi_m(\mathbf{r}) d^3\mathbf{r}. \quad (5)$$

In this paper, we assume the optical structure has only one dispersive material with negligible loss. This assumption is consistent with the previous studies of dispersive PCs [37–43], where only one dispersive material with negligible loss is considered. With these assumptions,  $\chi(\mathbf{r}, \omega)$  in Equation (5) can be written as  $\chi(\mathbf{r}, \omega) = X_F + X(\omega)\theta(\mathbf{r})$ , where  $X_F$  is a real constant value,  $X(\omega)$  is a real function of  $\omega$ , and  $\theta(\mathbf{r})$  is a dimensionless periodic function of  $\mathbf{r}$  describing the position of the dispersive material. The constant  $X_F$  is added to the dielectric function so that one can have additional freedom in choosing the backbone structure. The function  $\theta(\mathbf{r})$  equals to 1 if  $\mathbf{r}$  pointing towards the position of dispersive material and zero otherwise. Introducing  $F_n = \omega_n f_n$ , we can write Equation (5) in a symmetrized form as

$$\frac{1}{\omega^2} F_n = \sum_m \frac{1}{\omega_n \omega_m} [\delta_{nm} + X_F J_{nm} + X(\omega) \theta_{nm}] F_m, \quad (6)$$

where  $J_{nm} = \frac{1}{V} \int_{unit\ cell} \phi_n^*(\mathbf{r}) \phi_m(\mathbf{r}) d^3\mathbf{r}$  and  $\theta_{nm} = \frac{1}{V} \int_{unit\ cell} \phi_n^*(\mathbf{r}) \theta(\mathbf{r}) \phi_m(\mathbf{r}) d^3\mathbf{r}$ . The index  $m$  in Equation (6) in principle runs over all of the basis functions of the dielectric backbone, and this is an extreme waste of computational efforts. We will use symmetry arguments to simplify Equation (6). Firstly, note that, Equation (3) can be written in the operator form as  $\mathcal{H}_{bb} \phi_m(\mathbf{r}) = (\omega_m^2/c^2) \phi_m(\mathbf{r})$ , where  $\mathcal{H}_{bb} = [1/\varepsilon_{bb}(\mathbf{r})] \nabla \times \nabla \times$ . The set of symmetry elements,  $\mathcal{G}$ , that keep  $\mathcal{H}_{bb}$  invariant [i.e.,  $\mathcal{G} \mathcal{H}_{bb} \mathcal{G}^{-1} = \mathcal{H}_{bb}$ ] forms a group,  $G(\mathcal{H}_{bb})$ , under the group theory [44]. The basis function is then can be identified with an additional symmetry label given by the irreducible representation (IR) of the group  $G(\mathcal{H}_{bb})$ . Denoting small Greek letters for the labels of IRs, the indices  $n$  and  $m$  now can

be replaced with a pair of labels  $(n, \alpha)$  and  $(m, \beta)$ , respectively. If the symmetry of  $\chi(\mathbf{r}, \omega)$  is the same as the symmetry of  $\varepsilon_{bb}(\mathbf{r})$  [i.e., the  $G(\mathcal{H}) = G(\mathcal{H}_{bb})$ , where  $\mathcal{H} = \{1/\varepsilon(\mathbf{r}, \omega)\} \nabla \times \nabla \times$ ], then the term  $\theta_{(n,\alpha)(m,\beta)} = \frac{1}{V} \int_{unit\ cell} \phi_{(n,\alpha)}^*(\mathbf{r})\theta(\mathbf{r})\phi_{(m,\beta)}(\mathbf{r})d^3\mathbf{r}$  in Equation (6),

can be written as  $\theta_{(n,\alpha)(m,\beta)} = \frac{1}{V} \int_{unit\ cell} \psi_{(n,\alpha)}^*(\mathbf{r})\psi_{(m,\beta)}(\mathbf{r})d^3\mathbf{r}$ ,

where  $\psi_{(n,\alpha)}(\mathbf{r}) = \sqrt{\theta(\mathbf{r})}\phi_{(n,\alpha)}(\mathbf{r})$  is the function with the same symmetry as  $\phi_{(n,\alpha)}(\mathbf{r})$ . Using the orthogonality of the basis functions of different IR, one can show that  $\theta_{(n,\alpha)(m,\beta)} = \frac{1}{V} \int_{unit\ cell} \psi_{(n,\alpha)}^*(\mathbf{r})\psi_{(m,\beta)}(\mathbf{r})d^3\mathbf{r} = \delta_{\alpha\beta}\theta_{(n,\alpha)(m,\alpha)}$  and  $J_{(n,\alpha)(m,\beta)} = \frac{1}{V} \int_{unit\ cell} \phi_{(n,\alpha)}^*(\mathbf{r})\phi_{(m,\beta)}(\mathbf{r})d^3\mathbf{r} = \delta_{\alpha\beta}J_{(n,\alpha)(m,\alpha)}$ . Consequently,

Equation (6) can be decoupled to different sets of equations, 
$$\sum_m \frac{1}{\omega_{(n,\alpha)(n,\alpha)}\omega_{(m,\alpha)(m,\alpha)}} [\delta_{(n,\alpha)(m,\alpha)} + X_F J_{(n,\alpha)(m,\alpha)} + X(\omega)\theta_{(n,\alpha)(m,\alpha)}]$$

$F_{(m,\alpha)(m,\alpha)} = (1/\omega^2)F_{(n,\alpha)(n,\alpha)}$ , which can be solved independently for each  $\alpha$ . Therefore, we need to keep only the basis functions of the same IR in Equation (6). As we will illustrate later, this will significantly reduce the matrix size and the computational time of the eigenproblem.

For PCs, there are two different kinds of symmetries, the translation symmetry and the point group symmetry. In the group theoretical terms, we say that  $G(\mathcal{H})$  is a direct product group between a translation group and a point group. These groups have their own sets of IRs. For translation group, each wavevectors in the first Brillouin Zone (BZ) constitute to a different IR [44]. Therefore, the modes of the PC with the same IR will have modes with the same wavevector and the same IR of the point group. The IR of the point groups are usually identified using the Mulliken's labels such as  $A_1, A_2, B_1, B_2$  etc. [10, 44]. For a detail discussion on the symmetry representations in PCs, see Refs. [10, 45–47].

Equation (6) can be written in a matrix form as  $\hat{I}(1/\omega^2)\mathbf{F} = [\hat{B} + X(\omega)\hat{\theta}]\mathbf{F}$ , where the elements of  $\hat{I}, \hat{B}, \hat{\theta}$  and  $\mathbf{F}$  are  $\delta_{nm}, [\delta_{nm} + X_F J_{nm}]/(\omega_n\omega_m), \theta_{nm}/(\omega_n\omega_m)$  and  $F_n$ , respectively. Rearranging this equation, we arrive at a eigenvalue problem for each distinct symmetry,  $\alpha$ ,

$$\hat{X}(\omega)\mathbf{F} = X(\omega)\mathbf{F}, \quad (7)$$

where  $\hat{X}(\omega) = \hat{\theta}^{-1}[(1/\omega^2)\hat{I} - \hat{B}]$  is defined as a *dielectric function operator*. Equation (7) represents an eigenvalue problem for the dielectric function operator with  $X(\omega)$  being the eigenvalue. A useful orthogonality relationship between any two eigenvectors  $\mathbf{F}_i$  and  $\mathbf{F}_j$

of the nondegenerate eigenvalues, can be obtained by multiplying Equation (7) with  $\hat{\theta}$ , and noting that the resulting problem is a generalized symmetric eigenvalue problem. The resulting orthogonality relationship is  $\mathbf{F}_j \cdot \hat{\theta} \mathbf{F}_i = \delta_{ij}$ .

There are at least two ways to solve for  $\omega$  from Equation (7). In general, for all forms of  $X(\omega)$ , one can employ a graphical method.

In this method, we first graph the eigenvalues of the operator  $\hat{X}(\omega)$ ,  $E_n(\omega)$ , as a function of  $\omega$ . The intersection between the curves  $E_n(\omega)$  and  $X(\omega)$  produce the desired eigenfrequencies of the DPN. If  $X(\omega)$  is a polynomial rational function, then Equation (7) can be solved as a polynomial eigenvalue problem. In this case, Equation (7) can be written as  $\frac{1}{\omega^2 D(\omega)} \{ \sum_r \omega^r \hat{A}_r \} \mathbf{F} = 0$ , where  $D(\omega)$  is the denominator

of  $X(\omega)$  and the matrix coefficients ( $\hat{A}_r$ ) are functions of  $\hat{B}$ ,  $\hat{\theta}$ , and  $\hat{I}$ . Consequently, for a non-singular  $D(\omega)$ , we arrive at a polynomial eigenvalue problem,

$$\hat{P}(\omega) \mathbf{F} = 0, \quad (8)$$

where  $\hat{P}(\omega) = \sum_n \omega^n \hat{A}_n$ . Equation (8) can be solved using the standard techniques of polynomial eigenvalue problem. A thorough study of the mathematical properties of the matrix polynomials and the corresponding solution to the eigenvalue problems can be found in Ref. [48].

In Table 1, we have tabulated the nonzero matrix coefficients of  $\hat{P}(\omega)$  for dielectric functions of a two-level quantum dot [49], polar crystals [39, 43], and Drude-like materials. The Drude like materials include metals [37, 38], semiconducting [51] and superconducting [41] constitutes. Similar to previous studies [38, 39, 43], we have neglected the imaginary part of the complex dielectric constant, for all cases of  $X(\omega)$  in Table 1. As we can see from the Table 1, for Drude like materials, we have linear and quadratic polynomials in  $\omega^2$ , with the absence and the presence of dissipation, respectively. For polar crystals,  $\hat{P}$  are quadratic and cubic in  $\omega^2$ , with the absence and presence the of dissipation, respectively. For quantum dots  $\hat{P}$  are quartic in  $\omega$ . It is also easy to show the matrix polynomials for other forms of  $X(\omega)$ . In the case of a Sellmeier dispersion [52], we have quadratic and cubic polynomials in  $\omega^2$ , when we keep one and two dispersion terms in the Sellmeier equation, respectively. For the case of silicon based devices, to model the entire response of bulk crystalline silicon to light over the wavelength range from 300 to 1000 nm, recently a new effective polynomial rational form of  $X(\omega)$  is proposed in Ref. [53]. Using the proposed  $X(\omega)$ , it can be shown

**Table 1.** Nonzero  $\hat{A}_r$  for DPNs made of two level quantum dots, polar crystals and Drude-like materials. Here  $g$ ,  $\varepsilon$ ,  $\tau$ ,  $\omega_T$ , and  $\omega_p$  are constant values.

Model	Nonzero $\hat{A}_r$
<u>Drude like</u> (no dissipation) $-\varepsilon\omega_p^2/\omega^2$	$\hat{A}_2 = \hat{B}$ $\hat{A}_0 = -\varepsilon\omega_p^2\hat{\theta} - \hat{I}$
<u>Drude like — with</u> <u>dissipation (<math>\gamma</math>)</u> $-\frac{\varepsilon\omega_p^2}{\omega^2+\gamma^2}$	$\hat{A}_4 = \hat{B}$ $\hat{A}_2 = \gamma^2\hat{B} - \varepsilon\omega_p^2\hat{\theta} - \hat{I}$ $\hat{A}_0 = -\gamma^2\hat{I}$
<u>Polar Crystals</u> (no dissipation) $\frac{\varepsilon\omega_T^2}{(\omega_T^2-\omega^2)}$	$\hat{A}_4 = \hat{B}$ $\hat{A}_2 = -\omega_T^2\hat{B} - \varepsilon\omega_T^2\hat{\theta} - \hat{I}$ $\hat{A}_0 = \omega_T^2\hat{I}$
<u>Polar Crystals — with</u> <u>dissipation (<math>\gamma</math>)</u> $\frac{\varepsilon\omega_T^2(\omega_T^2-\omega^2)}{(\omega_T^2-\omega^2)^2+\gamma^2\omega^2}$	$\hat{A}_6 = \hat{B}$ $\hat{A}_4 = (\gamma^2 - 2\omega_T^2)\hat{B} - \varepsilon\omega_T^2\hat{\theta} - \hat{I}$ $\hat{A}_2 = \omega_T^4\hat{B} + \varepsilon\omega_T^4\hat{\theta} - (\gamma^2 - 2\omega_T^2)\hat{I}$ $\hat{A}_0 = -\omega_T^4\hat{I}$
<u>Two Level</u> <u>Quantum Dots</u> $\frac{g(\omega-\omega_0)\tau}{1+[(\omega-\omega_0)\tau]^2}$	$\hat{A}_4 = \tau^2\hat{B};$ $\hat{A}_3 = g\tau\hat{\theta} - 2\omega_0\tau^2\hat{B};$ $\hat{A}_2 = (1 + \omega_0^2\tau^2)\hat{B} - g\omega_0\tau\hat{\theta} - \tau^2\hat{I};$ $\hat{A}_1 = 2\omega_0\tau^2\hat{I};$ $\hat{A}_0 = -(1 + \omega_0^2\tau^2)\hat{I}$

that the corresponding matrix polynomial for silicon is a 5th degree polynomial in  $\omega^2$ .

If we assume the perturbation  $\chi(\mathbf{r}, \omega)$  is small, then the off diagonal elements of  $\hat{B}$ ,  $\hat{\theta}$ , and  $\hat{I}$  can be neglected, and the frequency of the  $m$ -th mode can be obtained from the scalar polynomial,

$$\sum_r \omega^r A_{r,mm} = 0, \tag{9}$$

where the scalar coefficients  $A_{r,mm}$  are function of diagonal elements of  $\hat{B}$ ,  $\hat{\theta}$ , and  $\hat{I}$ . Also, in this case, the corresponding matrix operator,  $\hat{X}(\omega) = \hat{\theta}^{-1}[(1/\omega^2)\hat{I} - \hat{B}]$  in Equation (7), reduces to a scalar operator,  $\theta_m^{-1}[(1/\omega^2) - B_m]$ , where  $\theta_m$  and  $B_m$  are the diagonal elements of  $\hat{B}$  and  $\hat{\theta}$ , respectively. It is worth to note that one can always attempt to

minimize the perturbation [i.e.,  $\chi(\mathbf{r}, \omega)$ ] by selecting an appropriate dielectric backbone structure [recall that  $\varepsilon(\mathbf{r}, \omega) = \varepsilon_{bb}(\mathbf{r}) + \chi(\mathbf{r}, \omega)$ ].

### 3. NUMERICAL EXAMPLE

For a purpose of illustration let's concentrate our discussion for the case of PCs constructed with frequency dependent dielectric materials. If we assume the basis functions are those of an empty lattice with  $\varepsilon_{bb}(\mathbf{r}) = 1$ , then the basis functions are given by plane waves with wavevectors  $\mathbf{k} + \mathbf{G}$ , where  $\mathbf{k}$  and  $\mathbf{G}$  are the Bloch and reciprocal lattice vectors, respectively. With these basis functions, Equation (8) accurately reproduces the generalized eigenvalue problem previously derived for specialized cases of metallic [37], and polar [39] PCs. Although, plane waves are the simplest form of the basis functions, it takes large number of plane waves to give accurate results. The set of basis functions of an empty lattice [ $\varepsilon_{bb}(\mathbf{r}) = 1$ ] is not the only choice for the set of basis functions. In fact, for a rapid convergence one should select the basis functions such that the corresponding  $\varepsilon_{bb}(\mathbf{r})$  minimizes the perturbation,  $\chi(\mathbf{r}, \omega)$ . If we assume the PC is constructed with a dispersive material of dielectric constant  $\varepsilon_d + X(\omega)$  in a background medium having a dielectric constant,  $\varepsilon_{background}$ , then the unit cell is described by  $\varepsilon(\mathbf{r}, \omega) = \varepsilon_{background} + [\varepsilon_d - \varepsilon_{background} + X(\omega)]\theta(\mathbf{r})$ . The choice of  $\varepsilon_{bb}(\mathbf{r})$  that minimizes the perturbation,  $\chi(\mathbf{r}, \omega)$  would be  $\varepsilon_{bb}(\mathbf{r}) = \varepsilon_{background}(\mathbf{r}) + [\varepsilon_d - \varepsilon_{background}]\theta(\mathbf{r})$ . Therefore, the basis functions that minimizes the perturbation are the modes of a PC constructed with frequency independent dielectric constants of  $\varepsilon_{background}$  and  $\varepsilon_d$ . As we will show in the numerical example, with such choice of  $\varepsilon_{bb}(\mathbf{r})$  and the corresponding set of basis functions, the scalar version of Equation (7) and the scalar polynomial in Equation (8) provide excellent approximations to the original matrix polynomial. We will also illustrate the significance role played by the basis function symmetry in the convergence of the calculation.

For a numerical illustration let's consider the  $E$ -polarization [electric field perpendicular to the periodic plane] of a 2D PC made of frequency dispersive circular rods in a frequency independent dielectric matrix. We will consider the rods to be made of polar crystals. Previously, polar crystals have been used in the investigations for the enhancement of the photonic band gap and investigation of co-existing polaritonic band gap in PCs [39, 40, 54, 55]. In Ref. [55], 2D PCs made of polar crystals are proposed for realization of terahertz metamaterials.

The real part of the dielectric function of a polar crystal [39, 43] with the presence of dissipation can be written as  $\varepsilon_\infty + X(\omega)$ , where

$X(\omega) = (\varepsilon_0 - \varepsilon_\infty) \frac{\omega_T^2(\omega_T^2 - \omega^2)}{(\omega_T^2 - \omega^2)^2 + \gamma^2 \omega^2}$  [43]. Here,  $\gamma$  is the absorption coefficient (dissipation),  $\omega_T$  is the transverse optical phonon frequency,  $\varepsilon_\infty$  and  $\varepsilon_0$  are asymptotic values of dielectric constant when the frequency is very large and small, respectively. For numerical evaluation let's consider the parameters of 2D PC made of Gallium arsenide (GaAs) [a polar crystal] rods in air, considered in Ref. [43]. The parameters are  $\varepsilon_0 = 12.66$ ,  $\varepsilon_\infty = 10.9$ ,  $\omega_T = 0.4$ , and  $r_{rod} = 0.472$ . Here  $r_{rod}$  is the ratio of rod radius to the lattice constant of the 2D PC,  $a$ . For  $\gamma = 0$ , the matrix polynomial is quadratic in  $\omega^2$  [Table 1] and has  $2N$  positive roots, where  $N$  is the matrix size [i.e., number of basis functions of the backbone]. For a nonzero  $\gamma$ , the matrix polynomial is cubic in  $\omega^2$  [Table 1], and the maximum number of roots is  $3N$ . For a given  $\mathbf{k}$ -vector, the solution to the polynomial eigenvalue problem [Equation (8)] is obtained using a "QZ factorization" method [48].

Figure 1(a) shows the graphical form of solution [Equation (7)] for an arbitrary wavevector in the first BZ, when  $\varepsilon_{bb}(\mathbf{r}) = 1 + (\varepsilon_\infty - 1)\theta(\mathbf{r})$  [PC backbone] is used for the basis functions. For a discussion we choose  $\mathbf{k} = (2\pi/a)[0.15 \ 0.35]$  and  $\gamma = 0.08$ . In the figure, the plots of  $X(\omega)$  and the eigenvalues  $E_n(\omega)$  of the dielectric function operator [i.e.,  $\widehat{X}(\omega)$ ] are shown for  $n = 1$  to 4. Here,  $n$  is the index of the eigenvalues of the dielectric function operator. The intersections between  $X(\omega)$  and  $E_n(\omega)$  yield the eigenfrequencies of the dispersive PC [i.e., the DPN]. The frequencies of dispersive PC are sorted in the ascending order and denoted with a band index. Note that  $n$  is not the same as the band index of the dispersive PC. For an example, in Fig. 1(a), there are four values of  $n$ , but there are six intersections (i.e., solutions correspond to six bands of the dispersive PC). It is also worth to note that, the maximum value of  $n$  is  $N$ , however the maximum value for the number of bands in a dispersive PC is  $2N$  (when  $\gamma = 0$ ) and  $3N$  (when  $\gamma \neq 0$ ).

Figure 1(b) compares the convergence of the calculation [Equation (8)] when  $\varepsilon_{bb}(\mathbf{r}) = 1$  [empty lattice backbone] and  $\varepsilon_{bb}(\mathbf{r}) = 1 + (\varepsilon_\infty - 1)\theta(\mathbf{r})$  [PC backbone] for band 4 of the dispersive PC [the triangle dot in Fig. 1(a)] of the dispersive PC. As it is obvious from the figure, the calculation with the basis functions of the PC backbone, exhibits much faster convergence compared to the convergence of calculation with the basis functions of the empty lattice backbone.

To see the effect of the symmetry of the basis functions in the convergence of calculation, let's compute the frequencies at the symmetrical  $\mathbf{k}$  vectors, with and without the symmetrical sorting of the basis functions. Symmetrical sorting refers to the sorting of the

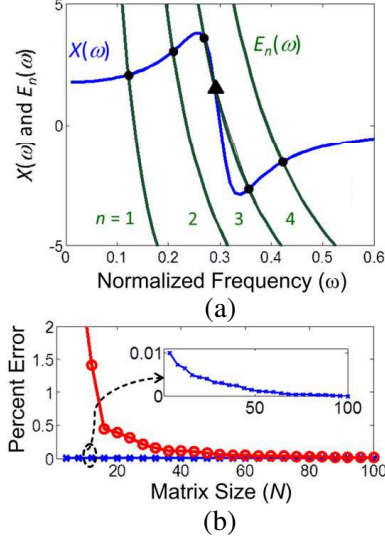


**Figure 1.** Graphical form of solution for frequencies of a 2D PC constructed with cylindrical rods [radius of the cylinder = 0.472] made of polar crystals.  $X(\omega)$  is the dielectric function of polar crystal with  $\varepsilon_0 = 12.66$ ,  $\varepsilon_\infty = 10.9$ ,  $\omega_T = 0.4$  and  $\gamma = 0.08$  (see text for the parameter definitions).  $E_n(\omega)$  is the eigenvalues of the dielectric function operator [Equation (7)]. (b) Percent error as a function of matrix size ( $N$ ) in Equation (8), when  $\varepsilon_{bb}(\mathbf{r}) = 1$  (i.e., empty lattice backbone) [red circles] and  $\varepsilon_{bb}(\mathbf{r}) = 1 + (\varepsilon_\infty - 1)\theta(\mathbf{r})$  (i.e., PC backbone) [blue crosses] for the fourth band [i.e., the triangle dot in (a)].

basis functions of the same IR, and only the basis functions of the same symmetry are included in constructing the matrices in Equation (8). Fig. 2(a) shows the convergence of calculation with the PC backbone at band 4 for the symmetrical  $\mathbf{k}$  vectors without the symmetrical sorting. The symmetrical  $\mathbf{k}$  vectors of a square lattice is shown in Fig. 2(b). Without the symmetry sorting, the calculated error as a function of matrix size [size of  $\hat{A}_r$  in Equation (8)], shows a “ladder” type of trends for symmetrical  $\mathbf{k}$  vectors [Fig. 2(a)], where the error does not change over some range of matrix sizes. From Fig. 2(a) we can see that, the range is wider for a  $\mathbf{k}$  vector with a higher symmetry than a  $\mathbf{k}$  vector with a lower symmetry. We also can see that, for a non-symmetrical  $\mathbf{k}$  vector, the range is zero [for e.g., see the  $\mathbf{A}$  vector]. This means that for a non-symmetrical  $\mathbf{k}$  vector, all the basis functions of the PC backbone contribute towards the convergence of the calculation, and

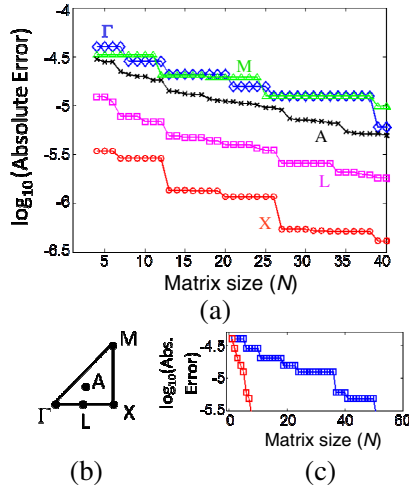


**Figure 2.** (a) Percent error as a function of matrix size ( $N$ ) in Equation (8), at different symmetrical  $\mathbf{k}$  vectors [band 4]. (b) Location of  $\mathbf{k}$  vectors in the irreducible BZ. (c) Percent error as a function of matrix size ( $N$ ) in Equation (8), at the band 4 of the  $\Gamma$  vector, with [red line] and without [blue line] the symmetrical sorting of the basis functions. Parameters of the PC for the both (a) and (c) are the same as in Fig. 1(a).

for symmetrical  $\mathbf{k}$  vectors only certain type of basis functions of the PC backbone contributes towards the convergence. From our discussion earlier, we can infer that these “certain type” of basis functions should possess the same symmetry. For an example, band 4 at  $\Gamma$  point has symmetry of  $B_1$  (label of the IR [10, 44–47]), and in Fig. 2(c) we showed the convergence of calculation at band 4 when only basis functions with the symmetries  $B_1$  are used in constructing the matrix coefficients of Equation (8) [i.e., with a symmetrical sorting]. As it is clear from the figure, only basis functions with the same symmetry contributes towards the convergence of the calculation, and the convergence is very rapid with the symmetrical sorting. To achieve an accuracy of  $\sim 10^{-6}$  in the absolute error,  $|\omega - \omega_{converged}|$ , at  $\Gamma$  point (band 4), only matrices with  $N = 7$  are required with the symmetrical sorting.

From Figs. 1(b), 2(a), and 2(c), we can see that with the PC backbone the convergence is very rapid, and results with high accuracy can be achieved, even with a very small  $N$ . We also found that, using the basis functions of the PC backbone, the scalar polynomials [Equation (9)] with  $\gamma$  values between 0 to 0.1 and  $\omega_T$

values 0 to 1, produces results with error less than 1 percent for the first twenty bands of all  $\mathbf{k}$  vectors in the first BZ.

Knowing the accuracy provided by the scalar polynomials, let's examine the analytical details provided by them. Fig. 3(a) shows the scalar polynomials for  $n = 1$  to 4 ( $n$  is index of eigenvalues  $E_n(\omega)$  of dielectric function operator). As we can see from these figures the scalar polynomials captures the essential features of the graphical form of solution in Fig. 1(a). When  $n = 1, 2$  and 4, there are only one intersections between  $X(\omega)$  and eigenvalues  $E_n(\omega)$  [Fig. 1(a)] and the corresponding polynomials [Fig. 3(a)] have only one root. When  $n = 3$ , there are three intersections between  $X(\omega)$  and  $E_n(\omega)$  [Fig. 1(a)], and the corresponding polynomial exhibits three roots [Fig. 3(a) and the inset].

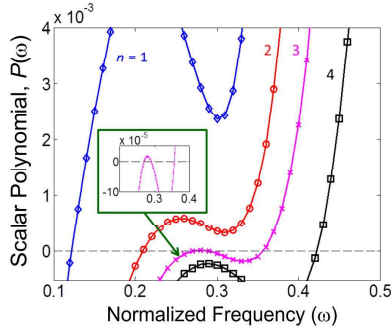


**Figure 3.** Scalar polynomials [Equation (9)] for the 2D PC with polar crystals [parameters as in Fig. 1(a)].

Let's analyze the asymptotic behavior of the scalar polynomial for the case of PCs made of polar crystals. The cubic-scalar polynomial [in  $\omega^2$ ] for polar crystals with nonzero dissipation ( $\gamma$ ) is  $P(\omega) = \omega^6 - \omega^4[\omega_n^2 + \omega_T^2(2 + \varepsilon\theta_n) - \gamma^2] - \omega^2[\omega_n^2(\gamma^2 - 2\omega_T^2) - \omega_T^4(1 + \varepsilon\theta_n)] - \omega_n^2\omega_T^4$ . The asymptotic solutions for  $P(\omega) = 0$ , when  $\omega_T \rightarrow 0$  and  $\omega_T \rightarrow \infty$  are  $\omega_n$  and  $\omega_n/\sqrt{1 + \varepsilon\theta_n}$ , respectively, where  $\varepsilon = \varepsilon_0 - \varepsilon_\infty$  and  $\theta_n = \theta_{nn}$ . To illustrate this we show exact solutions, together with the asymptotic lines for  $\gamma = 0.08$ ,  $n = 2$  in Fig. 4(a). When  $\gamma = 0$ , we have quadratic polynomial in  $\omega^2$  [Table 1],  $P(\omega) = \omega^4 - \omega^2[\omega_n^2 + \omega_T^2(1 + \varepsilon\theta_n)] + \omega_n^2\omega_T^2$ , with two positive solutions for  $\omega$ ,  $\omega_1$  and  $\omega_2$  [ $\omega_2 > \omega_1$ ]. The asymptotic solutions for  $\gamma = 0$ , when  $\omega_T \rightarrow 0$  and  $\omega_T \rightarrow \infty$  are  $\omega_1 \rightarrow 0$  [ $\omega_2 \rightarrow \omega_n$ ] and  $\omega_1 \rightarrow \omega_n/\sqrt{1 + \varepsilon\theta_n}$  [ $\omega_2 \rightarrow \omega_T\sqrt{1 + \varepsilon\theta_n}$ ], respectively. Another interesting asymptotic solution is for  $\omega_n \gg \omega_T$ , which yields  $\omega \rightarrow \omega_T$  [to obtain this divide  $P(\omega)$  for  $\gamma = 0$  with  $\omega_T^4$  and take the limit  $\omega_n/\omega_T \rightarrow \infty$ ]. This solution is independent of  $\theta_n$  [i.e., independent of

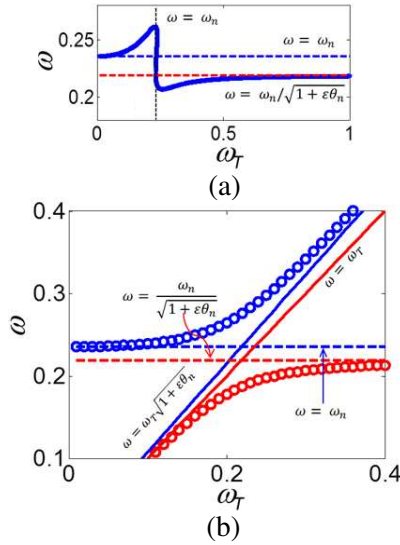


**Figure 4.** Normalized frequency  $\omega$  as a function of transversal phonon frequency,  $\omega_T$  for the 2D PC of polar crystals [parameters as in Fig. 1(a) with  $n = 2$ ] with dissipation (a)  $\gamma = 0.08$  and (b)  $\gamma = 0$ . In (a) [(b)], thick line [the circles] represents the solution to the scalar polynomial.

$\mathbf{k}$  vector], and therefore explains the appearance of many dispersionless bands (flat bands) when  $\omega = \omega_T$ , in the photonic band structure [i.e.,  $\omega$ - $\mathbf{k}$  relationship] of the 2D PC made of polar crystals [39, 40, 43, 54, 55]. The exact solutions, together with the asymptotic lines are shown for  $\gamma = 0$ ,  $n = 2$  in Fig. 4(b).

#### 4. SUMMARY

In summary, we have presented a new and efficient approach for the eigenvalue decompositions of a dispersive optical nanostructure. In the proposed method, we split the dielectric function of the dispersive PC into two components. One component has a non-dispersive dielectric function and the other has the dispersive portion of the dielectric function. The geometry described by the non-dispersive dielectric function is defined as a backbone structure. To solve the entire problem, we first solve the modes of the backbone structure. In the second step, we use these modes as basic functions to solve the modes of the dispersive optical nanostructure [via the eigenvalue problem

of the dielectric function operator (Equation (7) or the polynomial eigenvalue problem, Equation (8)). If we select a backbone structure that minimizes the frequency perturbation of the dielectric function of the dispersive PC, then large portion of the problem is already solved in the first step and therefore, rapid convergence can be achieved in the second step [i.e., in solving Equations (7)–(8)]. Only few modes [modes with the same symmetry] of the backbone structure are necessary to construct the matrices in Equations (7) and (8). Indeed, by numerical example we showed that for the particular case of a two-dimensional photonic crystal made of polar crystals, scalar polynomial [which is a result of Equation (8) with only one mode of the backbone photonic crystal] yields accurate eigenfrequencies.

The presented approach is general as it can handle any form of dielectric function as oppose to the previous direct method studies, where only specific forms of dielectric functions are assumed. Further, the approach is capable of producing semi-analytical descriptions for the eigenfrequencies of the dispersive optical nanostructures.

## REFERENCES

1. Cusack, M. A., P. R. Briddon, and M. Jaros, “Absorption spectra and optical transitions in InAs/GaAs self-assembled quantum dots,” *Phys. Rev. B*, Vol. 56, 4047–4050, 1997.
2. Politano, A., R. G. Agostino, E. Colavita, V. Formoso, and G. Chiarello, “Electronic properties of self-assembled quantum dots of sodium on Cu(1 1 1) and their interaction with water,” *Surf. Sci.*, Vol. 601, 2656–2659, 2007.
3. Politano, A., A. R. Marino, V. Formoso, D. Farías, R. Miranda, and G. Chiarello, “Evidence for acoustic-like plasmons on epitaxial graphene on Pt(111),” *Phys. Rev. B*, Vol. 84, 033401, 2011.
4. Borca, B., S. Barja, M. Garnica, M. Minniti, A. Politano, J. M. Rodríguez-García, J. J. Hinarejos, D. Farías, A. L. Vázquez de Parga, and R. Miranda, “Electronic and geometric corrugation of periodically rippled, self-nanostructured graphene epitaxially grown on Ru(0001),” *New J. Phys.*, Vol. 12, 093018, 2010.
5. Ariga, K., A. Vinu, Y. Yamauchi, Q. Ji, and J. P. Hill, “Nanoarchitectonics for mesoporous materials,” *Bull. Chem. Soc. Jpn.*, Vol. 85, 1–32, 2012.
6. Xuan, W., C. Zhu, Y. Liu, and Y. Cui, “Mesoporous metal-organic framework materials,” *Chem. Soc. Rev.*, Vol. 41, 1677–1695, 2012.
7. John, S., “Strong localization of photons in certain disordered

- dielectric superlattices,” *Phys. Rev. Lett.*, Vol. 58, 2486–2489, 1987.
8. Yablonovitch, E., “Inhibited spontaneous emission in solid-state physics and electronics,” *Phys. Rev. Lett.*, Vol. 58, 2059–2062, 1987.
  9. Joannopoulos, J. D., R. D. Meade, and J. N. Winn, *Photonic Crystals: Moding The Flow of Light*, Princeton University Press, Princeton, NJ, 1995.
  10. Sakoda, K., *Optical Properties of Photonic Crystals*, Springer, New York, 2001.
  11. Smith, D. R., J. B. Pendry, and M. C. K. Wiltshire, “Metamaterials and negative refractive index,” *Science*, Vol. 305, 788–792, 2004.
  12. Liu, Y. and X. Zhang, “Metamaterials: A new frontier of science and technology,” *Chem. Soc. Rev.*, Vol. 40, 2494–2507, 2011.
  13. Kosaka, H., T. Kawashima, A. Tomita, M. Notomi, T. Tamamura, T. Sato, and S. Kawakami, “Superprism phenomena in photonic crystals,” *Phys. Rev. B*, Vol. 58, R10096–R10099, 1998.
  14. Meier, M., A. Mekis, A. Dodabalapur, A. Timko, R. E. Slusher, J. D. Joannopoulos, and O. Nalamasu, “Laser action from two-dimensional distributed feedback in photonic crystals,” *Appl. Phys. Lett.*, Vol. 74, 7–9, 1999.
  15. Politano, A., “Influence of structural and electronic properties on the collective excitations of Ag/Cu(111),” *Plasmonics*, Vol. 7, 131–136, 2012. Ref. [7].
  16. Deubel, M., G. Freymann, M. Wegener, S. Pereira, K. Busch, and C. M. Soukoulis, “Direct laser writing of three-dimensional photonic-crystal templates for telecommunications,” *Nat. Mater.*, Vol. 3, 444–447, 2004.
  17. Chan, C. T., Q. L. Yu, and K. M. Ho, “Order-N spectral method for electromagnetic waves,” *Phys. Rev. B*, Vol. 51, 16635, 1995.
  18. Taflove, A. and S. C. Hagness, *Computational Electrodynamics: The Finite-difference Time-domain Method*, 3rd edition, Artech House, Inc., Norwood, 2005.
  19. Pendry, J. B., “Photonic band structures,” *J. Mod. Opt.*, Vol. 41, 209–229, 1994.
  20. Stefanou, N., V. Yannopoulos, and A. Modinos, “Heterostructures of photonic crystals: Frequency bands and transmission coefficients,” *Comp. Phys. Comm.*, Vol. 113, 49–77, 1998.
  21. Li, Z. Y. and L. L. Lin, “Photonic band structures solved by a plane-wave-based transfer-matrix method,” *Phys. Rev. E*, Vol. 67,

- 046607, 2003.
22. Deinega, A., S. Belousov, and I. Valuev, "Hybrid transfer-matrix FDTD method for layered periodic structures," *Opt. Lett.*, Vol. 34, 860–862, 2009.
  23. Hsue, Y.-C. and T.-J. Yang, "Applying a modified plane-wave expansion method to the calculations of transmissivity and reflectivity of a semi-infinite photonic crystal," *Phys. Rev. E*, Vol. 70, 016706, 2004.
  24. Shi, S., C. Chen, and D. W. Prather, "Revised plane wave method for dispersive material and its application to band structure calculations of photonic crystal slabs," *Appl. Phys. Lett.*, Vol. 86, 043104, 2005.
  25. Gu, B.-Y., L.-M. Zhao, and Y.-C. Hsue, "Applications of the expanded basis method to study the properties of photonic crystals with frequency-dependent dielectric functions and dielectric losses," *Physics Letters A*, Vol. 355, 134–141, 2006.
  26. Yuan, J. and Y. Y. Lu, "Photonic bandgap calculations with Dirichlet-to-Neumann maps," *J. Opt. Soc. Am. A*, Vol. 23, 3217–3222, 2006.
  27. Yuan, J., Y. Y. Lu, and X. Antoine, "Modeling photonic crystals by boundary integral equations and Dirichlet-to-Neumann maps," *J. Comp. Phys.*, Vol. 227, 4617–4629, 2008.
  28. Ho, K.-M., C. T. Chan, and C. M. Soukoulis, "Existence of a photonic gap in periodic dielectric structures," *Phys. Rev. Lett.*, Vol. 65, 3152–3155, 1990.
  29. Johnson, S. G. and J. D. Joannopoulos, "Block-iterative frequency-domain methods for Maxwell's equations in a planewave basis," *Opt. Exp.*, Vol. 8, 173–190, 2001.
  30. Notomi, M., "Theory of light propagation in strongly modulated photonic crystals: Refractionlike behavior in the vicinity of the photonic band gap," *Phys. Rev. B*, Vol. 62, 10696–10705, 2000.
  31. Foteinopoulou, S. and C. M. Soukoulis, "Electromagnetic wave propagation in two-dimensional photonic crystals: A study of anomalous refractive effects," *Phys. Rev. B*, Vol. 72, 165112, 2005.
  32. Jiang, W., R. T. Chen, and X. Lu, "Theory of light refraction at the surface of a photonic crystal," *Phys. Rev. B*, Vol. 71, 245115, 2005.
  33. Santamaría, F. G., J. F. G. López, P. V. Braun, and C. López, "Optical diffraction and high-energy features in three-dimensional photonic crystals," *Phys. Rev. B*, Vol. 71, 195112, 2005.
  34. Serebryannikov, A. E., T. Magath, and K. Schuenemann, "Bragg

- transmittance of *s*-polarized waves through finite-thickness photonic crystals with a periodically corrugated interface,” *Phys. Rev. E*, Vol. 74, 066607, 2006.
35. Li, Z. Y., L. L. Lin, and Z. Q. Zhang, “Spontaneous emission from photonic crystals: Full vectorial calculations,” *Phys. Rev. Lett.*, Vol. 84, 4341–4344, 2000.
  36. Zhou, Y. S., X. H. Wang, B. Y. Gu, and F. H. Wang, “Photonic band gap effects on spontaneous emission lifetimes of an assembly of atoms in two-dimensional photonic crystals,” *Phys. Rev. E*, Vol. 72, 017601, 2005.
  37. Kuzmiak, V., A. A. Maradudin, and F. Pincemin, “Photonic band structures of two-dimensional systems containing metallic components,” *Phys. Rev. B*, Vol. 50, 16835–16844, 1994.
  38. Kuzmiak, V. and A. A. Maradudin, “Photonic band structures of one- and two-dimensional periodic systems with metallic components in the presence of dissipation,” *Phys. Rev. B*, Vol. 55, 7427–7444, 1997.
  39. Kuzmiak, V., A. A. Maradudin, and A. R. McGurn, “Photonic band structures of two-dimensional systems fabricated from rods of a cubic polar crystal,” *Phys. Rev. B*, Vol. 55, 4298–4311, 1997.
  40. Zhang, W., A. Hu, X. Lei, N. Xu, and N. Ming, “Photonic band structures of a two-dimensional ionic dielectric medium,” *Phys. Rev. B*, Vol. 54, 10280–10283, 1996.
  41. Lee, W. M., P. M. Hui, and D. Stroud, “Propagating photonic modes below the gap in a superconducting composite,” *Phys. Rev. B*, Vol. 51, 8634–8637, 1995.
  42. Raman, A. and S. Fan, “Photonic band structure of dispersive metamaterials formulated as a hermitian eigenvalue problem,” *Phys. Rev. Lett.*, Vol. 104, 087401, 2010.
  43. Toader, O. and S. John, “Photonic band gap enhancement in frequency-dependent dielectrics,” *Phys. Rev. E*, Vol. 70, 046605, 2004.
  44. Inui, T., Y. Tanabe, and Y. Onodera, *Group Theory and Its Application in Physics*, Springer, Berlin, 1996.
  45. Alagappan, G., X. W. Sun, and H. D. Sun, “Symmetries of the eigenstates in an anisotropic photonic crystal,” *Phys. Rev. B*, Vol. 77, 195117, 2008.
  46. López-Tejiera, F., T. Ochiai, K. Sakoda, and J. Sánchez-Dehesa, “Symmetry characterization of eigenstates in opal-based photonic crystals,” *Phys. Rev. B*, Vol. 65, 195110, 2002.
  47. Sakoda, K., N. Kawai, T. Ito, A. Chutinan, S. Noda, T. Mitsuyu,

- and K. Hirao, “Photonic bands of metallic systems. I. Principle of calculation and accuracy,” *Phys. Rev. B*, Vol. 64, 045116, 2001.
48. Gohberg, I., P. Lancaster, and L. Rodman, *Matrix Polynomials*, Academic Press, London, 1982.
  49. Yariv, A., *Introduction to Theory and Applications of Quantum Mechanics*, John Wiley & Sons Inc., 1982.
  50. Kittel, C., *Introduction to Solid State Physics*, 7th Edition, Wiley, 1995.
  51. Halevi, P. and F. Ramos-Mendieta, “Tunable photonic crystals with semiconducting constituents,” *Phys. Rev. Lett.*, Vol. 85, 1875, 2000.
  52. Weber, M. J., *Handbook of Optical Materials*, Chap. 13, CRC Press, 2002.
  53. Deinega, A. and S. John, “Effective optical response of silicon to sunlight in the finite-difference time-domain method,” *Opt. Lett.*, Vol. 37, 112–114, 2012.
  54. Ribbing, C. G., H. Högström, and A. Rung, “Studies of polaritonic gaps in photonic crystals,” *Appl. Opt.*, Vol. 45, 1575–1582, 2006.
  55. Foteinopoulou, S., M. Kafesaki, E. N. Economou, and C. M. Soukoulis, “Two-dimensional polaritonic photonic crystals as terahertz uniaxial metamaterials,” *Phys. Rev. B*, Vol. 84, 035128, 2011.